Orthopaedics Section

Role of Hyaluronic Acid in Post-traumatic Osteoarthritis: Experimental Validation in a Rat Model

CHUNPEI OU¹, CHANGCHUN ZENG², PENGFEI ZHANG³, PENGFEI CHEN⁴, JINQI SONG⁵, GUANGMING LI⁶, YIKUN ZHAO⁷, ZHE CHENG⁸



ABSTRACT

Introduction: The pathogenesis of Post-traumatic Osteoarthritis (PTOA) remains incompletely understood. Although Hyaluronic Acid (HA) is widely used in the clinical management of Osteoarthritis (OA), its dynamic changes and mechanistic role in PTOA progression require further investigation.

Aim: To characterise the dynamic changes of HA concentration in synovial fluid and serum during post-traumatic Knee OA (KOA) development using a rat model.

Materials and Methods: The present Animal Randomised Controlled Trial (Animal RCT) was conducted in the laboratory of Longhua Central Hospital, Shenzhen, Guangdong Province, China, from August 2022 to July 2024. The present study utilised 36 male Sprague-Dawley rats (two-month-old, 320±20g). Rats were randomised into a sham control group (n=18; skin incision only) and Anterior Cruciate ligament Transection (ACLT) model group (n=18). Six subgroups (A-F) were established according to observation time points (postoperative days 7, 14, 21, 28, 70, and 98), each comprising three model and three control rats. Experimental procedures were temporally randomised, with collection of: Right hind-knee synovial fluid and serum

for Enzyme-Linked Immunosorbent Assays (ELISA), right hind-knee joint specimens for safranin O-fast green staining and immunohistochemical analysis of CD68+ macrophage infiltration. Statistical analyses employed linear regression curve fitting, descriptive statistics {mean±Standard Deviation (SD)}, Analysis of Variance (ANOVA), and Student's t-test. A p-value <0.05 was considered significant.

Results: Experimental groups exhibited progressive decline in synovial HA concentration with disease progression (p=0.028), reaching nadir levels at postoperative Day 70 (synovial fluid: 5.113±0.2478 ng/mL; serum: 6.671±0.8706 ng/mL), followed by modest recovery (Days 71-98). HA dynamics demonstrated significant negative correlations with IL-1 levels expression (r=-0.5335, p<0.05).

Conclusion: Post-traumatic joint instability induces sustained HA depletion (≤Day 70), potentially accelerating cartilage matrix degradation through Matrix Metalloproteinases (MMP)-13 upregulation and IL-1-mediated inflammatory cascades. These findings identify promising therapeutic targets for early PTOA intervention.

Keywords: Anterior cruciate ligament injuries, Cartilage, Degenerative joint disease

INTRODUCTION

The OA is a prevalent degenerative joint disease commonly found in middle-aged and elderly populations. The knee joint is one of the most frequently affected, with inflammatory responses and cartilage degeneration leading to severe pain and functional impairment. In China, OA affects >140 million individuals, with KOA being most prevalent (46.3% in adults aged >40 years) [1,2]. PTOA, defined as secondary joint degeneration triggered by articular trauma (e.g., fractures, cartilage/ligament injuries) [3], is characterised by progressive cartilage loss, subchondral sclerosis, osteophytes, and synovitis [4]. Its substantial burden includes 5.6 million US patients and \$3.2B annual costs from early joint replacements [5]. PTOA accounts for over 12% of all OA cases, and the knee, due to its high-load bearing nature, is a predominant site for PTOA development [6]. Trauma is a significant factor in the progression of knee PTOA, particularly Anterior Cruciate Ligament (ACL) ruptures, which often trigger its onset [7,8]. MMP-13 is a core effector in PTOA pathogenesis, driving joint degeneration via direct Extracellular Matrix (ECM) degradation [9], HA dysfunction [10], and inflammatory amplification [11]. The proinflammatory cytokine IL-1B orchestrates catabolic cascades by: 1) inducing synovial release of TNF-α/IL-6 to promote MMP-13-mediated cartilage destruction [12,13]; 2) disrupting subchondral bone homeostasis through aberrant osteoclast activation [14]; and 3) suppressing HA synthesis via HAS2 downregulation in synoviocytes [15], creating a feedforward loop of tissue damage. Previous studies highlight the need for further research into the mechanisms regulating lubricin and HA following joint injury, as well as their impact on joint homeostasis-including whether lubricin could serve as a biomarker for PTOA [16,17]. Although existing evidence confirms a strong correlation between HA metabolic dysregulation, proinflammatory cytokine cascades, and OA progression, the precise regulatory role of HA dynamics in the early-stage joint microenvironment of PTOA and its effect on cartilage degeneration remain unclear.

On the other hand, while exogenous HA supplementation is clinically used to treat OA, the optimal therapeutic time window for delaying disease progression or preventing further deterioration has not been established. By establishing temporal correlations between HA dynamics and disease severity (quantified via cartilage-degrading enzyme MMP-13 and proinflammatory cytokine IL-1), The present study further dissect HA-driven degenerative cascades to identify early biomarkers and elucidate mechanistic underpinnings of PTOA pathogenesis.

Thus, the present study aimed to dynamically track compartmentspecific changes in HA concentration within synovial fluid (local joint microenvironment) and serum (systemic circulation) across defined stages of PTOA progression in a rat model.

MATERIALS AND METHODS

The present animal RCT was conducted in the laboratory of Longhua Central Hospital, Shenzhen, Guangdong Province, China, from August 2022 to July 2024. This study was approved by the

Animal Experimentation Ethics Committee of Guangdong Medical University with Approval number GDY2102496 and adheres to the ethical guidelines of the Declaration of Helsinki. This study was supported by the Scientific Research Projects of Medical and Health Institutions of Longhua District, Shenzhen, Guangdong Province, China (Grant No. 2022006).

Inclusion criteria: Subjects were 36 healthy male Sprague Dawley rats, aged 2 months, weighing (320±20) g.

Exclusion criteria: Female SD rats were excluded. Male SD rats weighing greater than 340 g or less than 320 g were excluded. Rats used in previous studies and diseased rats were excluded.

Sample size calculation: Sample size was calculated for the primary outcome (CD68+ H-Score difference) using Cohen's effect size for independent samples. Based on $\alpha{=}0.05~(Z_{1.}~\alpha/_{2}{=}1.96),\,80\%$ power ($\beta{=}0.20,\,Z_{1.}~\beta{=}0.84),$ pilot data (pooled SD $\sigma{=}65.2),$ and a clinically significant difference ($\Delta{=}70)$, the formula yielded n ≈13.6 /group. Accounting for potential attrition, a minimum of 14 rats/group was required. To ensure power and exceed the recommended 12.5% safety margin [18], 18 rats/group (Sham/ACLT) were enrolled, with three rats/subgroup per time point.

Study Procedure

Thirty-six healthy adult male Sprague-Dawley rats (320±20 g), procured from the Guangdong Medical Laboratory Animal Centre (Licence SCXK (Yue) 2013-0002), and were maintained under standard laboratory conditions with unrestricted access to food and water and a 12-hour light-dark cycle. Using a digital randomisation method [19], the rats were divided into two primary groups: the ACLT group (n=18), which underwent ACLT of the right hind knee, and the Sham group (n=18), which received an identical surgical procedure without ligament transection to establish a PTOA model. These groups were further stratified into six subgroups (A-F) based on postoperative time points via digital random allocation, with each subgroup containing three rats from the ACLT group and three from the Sham group (n=6 per subgroup). The postoperative intervals for sample collection were Day 7 (group A), Day 14 (group B), Day 21 (group C), Day 28 (group D), Day 70 (group E), and Day 98 (group F). At the designated time points, synovial fluid from the right hind knee joint and blood from the orbital sinus were collected using sterile Eppendorf tubes. Following sample collection, the animals were euthanised, and the right hind limbs were dissected. The knee joints were isolated and cleared of excess soft-tissue for subsequent histological sectioning and analysis.

Articular cartilage pathology was evaluated using the Mankin scoring system [20], which assesses four parameters: cartilage structure (0-6 points), chondrocyte distribution (0-3 points), proteoglycan loss based on Safranin O staining intensity (0-4 points), and tidemark integrity (0-1 point). Tissue sections were fixed in 10% formalin, paraffin-embedded, and sliced into 4 μm sections, followed by Safranin O- Fast Green staining for microscopic evaluation.

To assess macrophage infiltration, Immunohistochemistry (IHC) targeting CD68 protein was performed. Antigen retrieval was conducted with citrate buffer (pH 6.0) at 95°C for 20 minutes. Sections were incubated overnight at 4°C with rabbit polyclonal anti-CD68 antibody (clone KP1, Servicebio #GB113109-100; 1:200 dilution in PBS), followed by HRP-conjugated secondary antibody and DAB chromogen detection (GB23303 kit). Nuclei were counterstained using Mayer's haematoxylin. CD68 expression was quantified via the H-score method, calculated as H-score= Σ (ixP_i), where i denotes staining intensity (0=negative, 1=weak, 2=moderate, 3=strong) and P_i the percentage of cells at each intensity. The final H-score ranged from 0 to 300, based on microscopic evaluation [21].

Two pathologists independently scored five randomly selected 200× magnification fields per section under blinded conditions. Inter-observer agreement was substantial, as indicated by Cohen's

 κ coefficient (κ =0.674; 95% CI: 0.560–0.788; *p*<0.001).

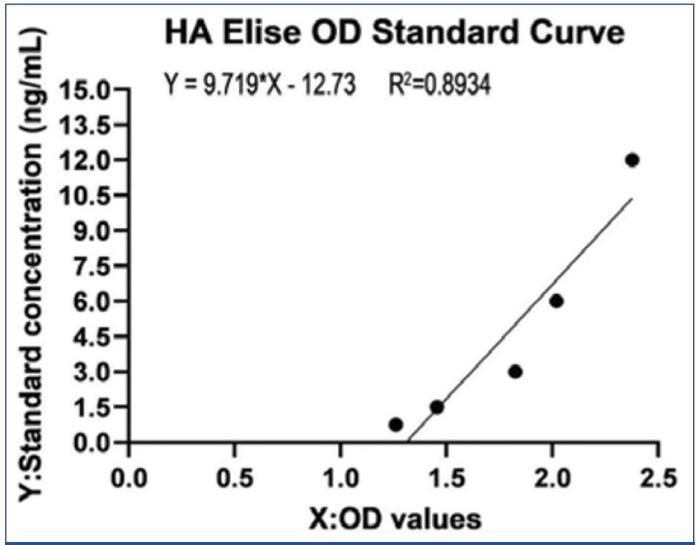
ELISA quantification: Serum and synovial fluid levels of HA, matrix metalloproteinase-13 (MMP-13), and Interleukin-1 (IL-1) were quantified using commercial ELISA kits (Shenzhen Leading Technology) according to the manufacturer's protocols. The specific kits used were: Rat IL-1(Cat. # ZK-R3136), Rat MMP-13 (Cat. # ZK-R3198), Rat HA (Cat. # LZ-R6783). All assays were performed in triplicate. Sample centrifugation steps were carried out using a Beckman Coulter OPTIMA XE-90 centrifuge.

STATISTICAL ANALYSIS

Statistical analyses used GraphPad Prism 9. Data are mean±SD. Pre-experiment body weights were compared by One-way ANOVA. Inter-group comparisons used One-way ANOVA with Tukey's post-hoc test (p<0.05 significance).

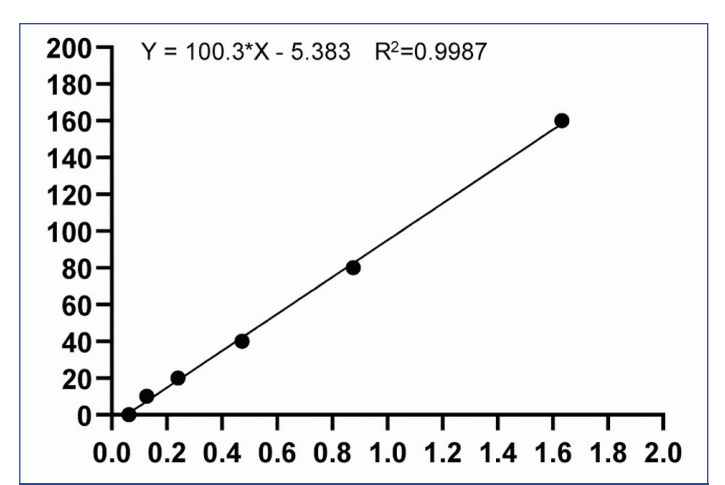
RESULTS

All groups demonstrated comparable baseline weights (range: 216.33-218.00 g; overall mean=217.06 \pm 1.75 g; ANOVA p=0.640); there were no statistically significant differences between the groups. HA ELISA standard curves were fitted using a linear regression model (R²=0.8934, p=0.0153, [Table/Fig-1]), indicating a strong linear relationship between HA standard concentrations and OD



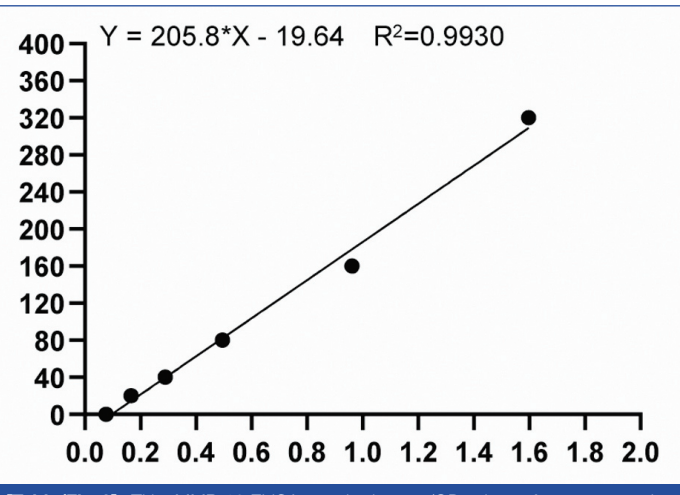
[Table/Fig-1]: Title: HA ELISA Standard Curve (OD Values of Rat Serum and Synovial Fluid).

X-axis: Measured OD Values; Y-axis: HA ELISA Standard Concentration (µg/mL); Regression: Equation: Y=9.719 x X-12.73, Goodness of Fit: R2=0.8934; Legend: Scatter points represent measured OD values of standards, Solid line indicates the linear regression. Linear regression analysis



[Table/Fig-2]: Title: IL-1 ELISA Standard Curve (OD Values of Rat Serum and Synovial Fluid); X-axis:

Measured OD Values; Y-axis: IL-1 ELISA Standard Concentration (pg/mL); Regression: Equation: Y=100.3*X - 5.383, Goodness of Fit: R²=0.9987; Legend: Scatter points represent measured OD values of standards, Solid line indicates the linear regression fit. Linear regression analysis (solid line). p<0.0001 values. IL-1ELISA standard curves followed a linear regression model (R 2 =0.9987, p<0.0001.[Table/Fig-2]), demonstrating a robust linear correlation between IL-1standard concentrations and OD values. MMP-13 ELISA standard curves were analysed via linear regression (R 2 =0.9930, p<0.0001, [Table/Fig-3]), confirming a significant linear association between MMP-13 standard concentrations and OD values.

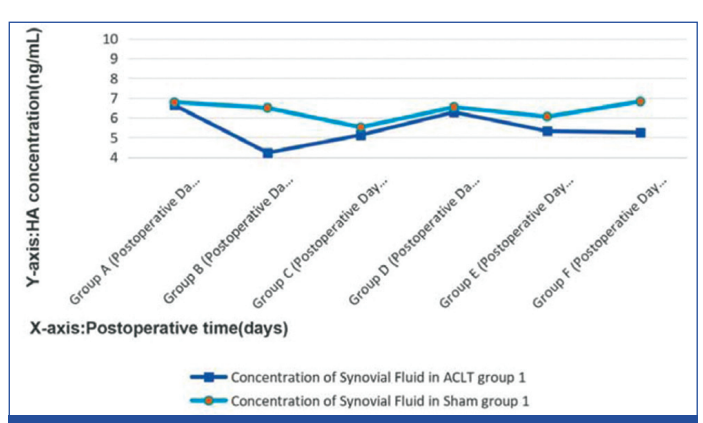


[Table/Fig-3]: Title: MMP-13 ELISA standard curve (OD values of rat serum and synovial fluid).

X-axis: Measured OD Values; Y-axis: MMP-13 ELISA Standard Concentration (pg/mL); Regression: Equation: $Y = 205.8^{+}X - 19.64 R^{2} = 0.9930$, Goodness of Fit: $R^{2} = 0.9930$; Legend: Scatter points represent.

The measured OD values of standards and the solid line indicate the linear regression fit. Linear regression analysis (solid line), p<0.0001

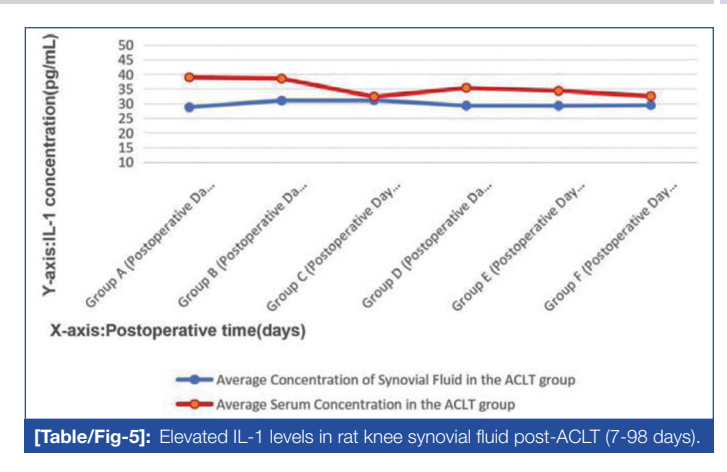
A comparative evaluation of synovial fluid concentrations in Sprague Dawley rats (groups A-F) revealed a statistically significant difference between ACLT group 1 and Sham group 1 (p=0.028), indicating distinct biochemical profiles as presented in [Table/Fig-4]. Over time, IL-1 levels in rat knee synovial fluid showed a gradual increase, with values expressed as mean±SD (pg/mL). Paired t-test analysis demonstrated notable differences across specific group comparisons: group A (38.93±5.51 pg/mL) versus group F (p=0.035), group B (38.81±3.80 pg/mL) versus group F (p=0.012), and group E (34.36±1.09 pg/mL) versus group F (p=0.009). Additionally, group B, compared to group E, yielded a significant difference (p=0.021), underscoring progressive changes in IL-1 concentrations across experimental conditions [Table/Fig-5].

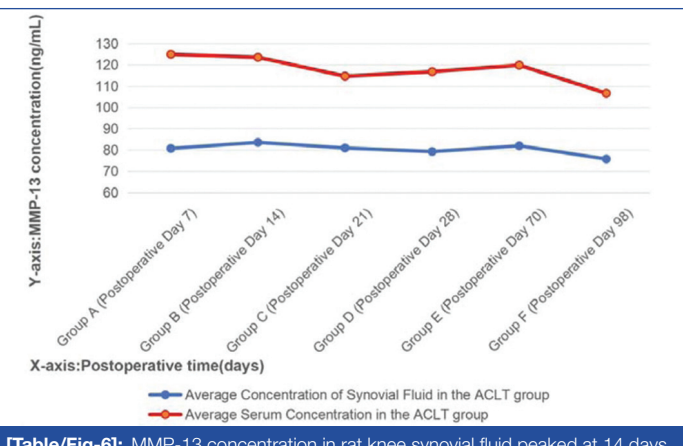


[Table/Fig-4]: Time-dependent changes in HA concentration in synovial fluid of ACLT-induced OA rats.

ACLT model (n=6/group). Related-samples Wilcoxon signed-rank test. ACLT group (p=0.028 < 0.05) vs sham group.

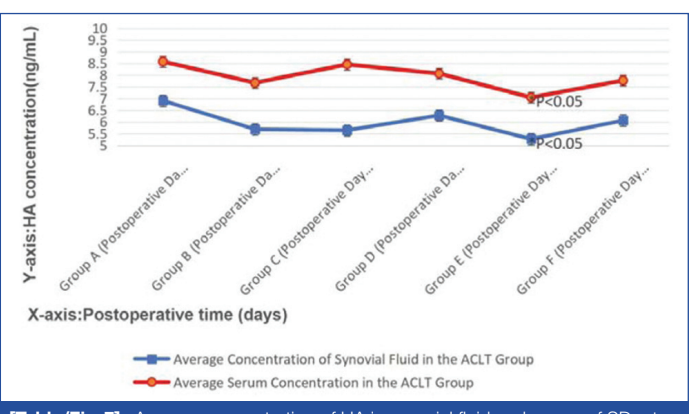
MMP-13 concentrations exhibited an increase by postoperative day 14, followed by a slight decrease by Day 98, as illustrated in [Table/Fig-6]. Statistical analysis using the paired t-test revealed significant differences when compared with the final (F) values across multiple groups: group A recorded 18.33 \pm 14.01 with a p-value of 0.024; group B showed 16.90 \pm 10.30 with a p-value of 0.010; and group E had 13.19 \pm 11.38 with a p-value of 0.036.





[Table/Fig-6]: MMP-13 concentration in rat knee synovial fluid peaked at 14 days post-ACLT.

HA concentrations reached their lowest point at postoperative day 70 (synovial fluid: 5.273 ± 0.422 ng/mL; serum: 7.047 ± 0.739 ng/mL; *p*<0.05 by ANOVA), with a mild recovery observed by Day 98 [Table/Fig-7]. One-way ANOVA indicated significant inter-group differences in HA concentrations for synovial fluid (F5,30=4.374, pp=0.0033) and serum (F5,30=2.874, pp=0.031). Tukey's post-hoc analysis revealed: Synovial fluid: group A > group E.



[Table/Fig-7]: Average concentration of HA in synovial fluid and serum of SD rats as measured by ELISA.

 $\{\Delta=1.60~\mu g/mL,~95\%~Cl~(0.30,~2.90),~pp=0.009\}; Serum:~group~A>group~E~\{\Delta=1.78~\mu g/mL,~95\%~Cl~(0.28,~3.28),~pp=0.014\};~group~A~showed~the~highest~concentrations~in~both~compartments,~group~E~the~lowest.~HA~dynamics~demonstrated~significant~negative~correlations~with~IL-1levels~expression~(r=-0.5335,~p<0.05).$

Cartilage proteoglycan loss (Safranin O-Fast Green). ACLT group: A=1, B=1, C=3, D=5, E=6, F=7. Data points represent individual samples (n=6/group). p<0.01 vs Sham by Mann-Whitney U test [Table/Fig-8,9].

Immunohistochemistry (IHC) analysis of CD68+ macrophage infiltration in synovial tissue revealed distinct cellular distribution, with CD68+ cells appearing as brown-stained regions against a haematoxylin counterstain background. Quantitative assessment



[Table/Fig-8]: Results of Safranin O-Fast Green staining on cartilage sections from the right hind knee joint in rats of the Sham groups at different time points. Sham group (receiving identical surgical exposure without ACL transection): Safranin O-Fast Green staining of rat posterior knee joints at postoperative Day 7 (A), Day 14 (B), Day 21 (C), Day 28 (D), Day 70 (E), and Day 98 (F). Scale bar: 200 μ m. Original magnification ×5.



[Table/Fig-9]: Results of Safranin O-Fast Green staining on cartilage sections from the right hind knee joint in rats of the ACLT groups at different time points. ACLT group (undergoing anterior cruciate ligament postoperative Day 7 (A), Day 14 (B), Day 21 (C), Day 28 (D), Day 70 (E), and Day 98 (F). Scale bar: 200µm. Original magnification ×5.Data points represent individual samples (n=6/group).

***p<0.01 vs Sham by Mann-Whitney U test

was performed using H-Score analysis across various groups subjected to ACLT. The scores were as follows: group A=33, group B=39, group C=42, group D=100, group E=210, and group F=100. All ACLT groups showed significantly higher H-Scores compared to the Sham group, with statistical significance marked at p<0.001.

surface defects following ACLT, with degeneration stabilising between Days 70 and 98, potentially due to reduced weight-bearing or inflammatory feedback. Synovial macrophage infiltration (CD68+) also increased over time in the ACLT group, while remaining minimal in sham-treated rats, confirming CD68 as a reliable marker [28,29].



[Table/Fig-10]: CD68+ macrophage infiltration in cartilage of the right hind knee joint in Sham groups. Sham group: CD68+ macrophages in rat posterior knee joints. (a-f) Immunohistochemical staining of sham group at postoperative Day 7 (a), Day 14 (b), Day 21 (c), Day 28 (d), Day 70 (e), and Day 98 (f). Scale bar: 200µm. Original magnification × 10 (b), Day 21 (c), Day 28 (d), Day 29 (d), Day 29 (f).



[Table/Fig-11]: CD68+ macrophage infiltration in cartilage of the right hind knee joint in ACLT. ACLT group: CD68+ macrophages in rat posterior knee joints. (a-f) Immunohistochemical staining of ACLT group at postoperative Day 7 (a), Day 14 (b), Day 21 (c), Day 28 (d), Day 70 (e), and Day 98 (f). Scale bar: 200μm. Original magnification ×5.median H-score: ACLT=71 vs. sham=15; Δ=56, p<0.001) (Mann-Whitney U=0.0).

Each group comprised six individual samples (n=6), with data represented as individual values; median and Interquartile Range (IQR) are indicated by horizontal lines in the corresponding figures [Table/Fig-10,11].

DISCUSSION

The present study observed that following ACLT in the right hind knee of rats, the IL-1 concentration in synovial fluid demonstrated a progressive increase from Day 7 to Day 98. Meanwhile, MMP-13 concentration was elevated in the early postoperative phase, broadly consistent with the findings of He XF et al., but gradually declined from Day 15 onward possibly due to restricted mobility in caged Sprague-Dawley rats, which may slow OA progression [22]. Regulatory feedback mechanisms could also contribute to these fluctuations. Additionally, serum MMP-13, likely originating from systemic sources rather than articular tissues, lacks diagnostic sensitivity and specificity for PTOA. Prior studies further support that NUMB Endocytic Adaptor Protein (NUMB) mitigates PTOA by downregulating Beta-Transducin Repeat Containing E3 Ubiquitin Protein Ligase (BTRC) and inhibiting the NF-κB pathway, as assessed via Safranin O-Fast Green staining [23-26], the present study employed this staining method. However, unlike previous studies [27], the present study included both experimental and sham-operated control groups, analysing SD rat knee joint sections from Day 7 to Day 98.

The present study highlights progressive cartilage deterioration including matrix loss, disorganised chondrocyte alignment, and

HA levels in synovial fluid and serum dropped sharply to their lowest point at Day 70, then recovered modestly by Day 98. This HA depletion likely results from cartilage breakdown, inflammation, and impaired HA metabolism, aligning with prior findings that HA inhibits the CB12-I–PI3K/AKT/NF- κB axis and reduces MMP-13 via CD44 [30,31]. Notably, HA concentrations inversely correlated with IL-1 levels, underscoring IL-1's role in disease progression. The data suggest that HA dynamics are key in early PTOA pathogenesis and that sodium hyaluronate administered at or before Day 70 may delay or prevent OA advancement, offering a promising therapeutic strategy [32,33].

However, no optimal treatment window exists. The present study found that HA nadir occurs at Day 70, suggesting that early sodium hyaluronate administration (prophylactically or at this critical juncture) may delay OA progression or prevent worsening. This provides a theoretical foundation for PTOA management.

Limitation(s)

The study faced several limitations. The sample size was relatively small due to the subgroup analysis, which may affect the generalisability of the findings. Its single-laboratory design also raises the possibility of selection bias, as animal characteristics, genetic backgrounds, or husbandry conditions might not be representative of other laboratories. Additionally, the follow-up period was limited, potentially restricting the ability to capture long-term outcomes or the natural progression of the condition under investigation.

CONCLUSION(S)

Progressive joint degeneration was associated with a significant decline in synovial HA concentration, reaching its lowest level during the subacute postoperative phase, followed by partial recovery in later stages. Critically, HA dynamics demonstrated a statistically significant inverse correlation with IL-1 expression levels, establishing that elevated IL-1 contributes fundamentally to HA depletion during disease progression. These findings highlight IL-1-driven inflammation as a key pathogenic mechanism underlying HA loss in PTOA, suggesting therapeutic strategies targeting this inflammatory pathway may preserve joint homeostasis.

REFERENCES

- [1] Li S, Wang Y, Zhang Y, Yi M, Yang Y, He J, et al. Prevalence and associated factors of knee osteoarthritis in a rural Chinese adult population: An epidemiological survey. Arthritis Res Ther. 2019;21(1):234.
- [2] Wang Y, Wluka AE, Simpson JA, Giles GG, Graves SE, de Steiger RN, et al. Body weight at early and middle adulthood, weight gain and persistent overweight from early adulthood are predictors of the risk of total knee and hip replacement for osteoarthritis. Ann Rheum Dis. 2020;79(5):583-89.
- [3] Loeser RF. Aging processes and the development of osteoarthritis. Nat Rev Rheumatol. 2016;12(7):392-402. Doi: 10.1038/nrrheum.2016.65.
- [4] Lotz MK, Kraus VB. New developments in osteoarthritis. Posttraumatic osteoarthritis: Pathogenesis and pharmacological treatment options. Arthritis Res Ther. 2010;12(3):211. Doi: 10.1186/ar3046.
- [5] Bank NC, Sanghvi P, Hecht CJ 2nd, Mistovich RJ. The epidemiology of posttraumatic osteoarthritis of the knee in the United States: An analysis of 948,853 patients from 2000 to 2022. J Am Acad Orthop Surg. 2024;32(7):e313e320. Doi: 10.5435/JAAOS-D-23-00662.
- [6] Brown TD, Johnston RC, Saltzman CL, Marsh JL, Buckwalter J. Posttraumatic osteoarthritis: A first estimate of incidence, prevalence, and burden of disease. J Orthop Trauma. 2006;20(10):739-44.
- [7] Alonso B, Bravo B, Mediavilla L, Gortazar AR, Forriol F, Vaquero J, et al. Osteoarthritis-related biomarkers profile in chronic anterior cruciate ligament injured knee. Knee. 2020;27(3):1230-38.
- [8] Li H, Chen C, Chen S. Posttraumatic knee osteoarthritis following anterior cruciate ligament injury: Potential biochemical mediators of degenerative alteration and specific biochemical markers. Biomed Rep. 2015;3(2):153-58.
- [9] Li X, Zhang Y, Chen Q, Liu H, Wang F, Wei L, et al. Collagenase-mediated ECM remodeling inpost-traumatic joint degeneration. Osteoarthritis Cartilage. 2023;31(7):891-903. Doi: 10.1016/j.joca.2023.03.010.
- [10] Zhang Q, Liu Y, Wang T, Chen L, Zhao H, Xu K, et al. Hyaluronan-based hydrogels preserve joint homeostasis through MMP-13 suppression. Int J Nanomedicine. 2024;19:1021-35. Doi: 10.2147/JJN.S452311.
- [11] Zhou D, Wei Y, Sheng S, Wang M, Su J, Wei Y, et al. MMP13-responsive siRNA delivery systems for precision PTOA therapy. Bioact Mater. 2024;35:198-212. Doi: 10.1016/j.bioactmat.2024.05.001.
- [12] Kapoor M, Martel-Pelletier J, Lajeunesse D, Pelletier JP, Fahmi H. Role of proinflammatory cytokines in the pathophysiology of osteoarthritis. Nat Rev Rheumatol. 2011;7(1):33-42. Doi: 10.1038/nrrheum.2010.196.
- [13] Wang X, Hunter DJ, Jin X, Ding C. The importance of IL-1 β and TNF- α , and the differential role of MMP-13 in the propagation of cartilage degradation in osteoarthritis. Osteoarthritis Cartilage. 2022;30(8):1058-68. Doi: 10.1016/j. joca.2022.04.008.

- [14] Kwan Tat S, Lajeunesse D, Pelletier JP, Martel-Pelletier J. Targeting subchondral bone for treating osteoarthritis: What is the evidence? Best Pract Res Clin Rheumatol. 2010;24(1):51-70. Doi: 10.1016/j.berh.2009.08.004.
- [15] Tamer TM. Hyaluronan and synovial joint: Function, distribution and healing. Interdiscip Toxicol. 2013;6(3):111-25. Doi: 10.2478/intox-2013-0019.
- [16] Peal BT, Gagliardi R, Su J, Fortier LA, Delco ML, Nixon AJ, et al. Synovial fluid lubricin and hyaluronan are altered in equine osteochondral fragmentation, cartilage impact injury, and full-thickness cartilage defect models. J Orthop Res. 2020;38(8):1826-35.
- [17] Watkins A, Fasanello D, Stefanovski D, Schurer S, Caracappa K, D'Agostino A, et al. Investigation of synovial fluid lubricants and inflammatory cytokines in the horse: A comparison of recombinant equine interleukin 1 beta-induced synovitis and joint lavage models. BMC Vet Res. 2021;17(1):189.
- [18] Festing MFW, Altman DG. Guidelines for the design and statistical analysis of experiments using laboratory animals. ILAR J. 2002;43(4):244-58.
- [19] Schulz KF, Chalmers I, Hayes RJ, Altman DG. Generation of allocation sequences in randomised trials: Chance, not choice. Lancet. 2002;359(9305):515-19.
- [20] Afara I, Prasadam I, Crawford R, Xiao Y, Oloyede A, Moody H, et al. Non-destructive evaluation of articular cartilage defects using Near-Infrared (NIR) spectroscopy in osteoarthritic rat models and its direct relation to Mankin score. Osteoarthritis Cartilage. 2012;20(11):1367-73. Doi: 10.1016/j.joca.2012.07.017.
- [21] Wen Z, Luo D, Wang S, Rong R, Evers BM, Jia L, et al. Deep Learning-Based H-Score quantification of immunohistochemistry-stained images. Mod Pathol. 2024;37(2):100398.
- [22] He XF, Li W, Zhu LM, Zhang JW, Wang Y, Li J, et al. Investigation for effects of iNOS on biological function of chondrocytes in rats with post-traumatic osteoarthritis. Eur Rev Med Pharmacol Sci. 2018;22(11):7140-47. Doi: 10.26355/eurrev_201811_16319.
- [23] Lv Z, Ding Y, Zhang W. NUMB attenuates posttraumatic osteoarthritis by inhibiting BTRC and inactivating the NF-kB pathway. J Orthop Surg Res. 2024;19(1):502.
- [24] Hu L, Luo D, Zhang H, He L. Polydatin inhibits IL-1β-mediated chondrocyte inflammation and ameliorates cartilage degradation: Involvement of the NF-κB and Wnt/β-catenin pathways. Tissue Cell. 2022;78:101865.
- [25] Lv Z, Sun D, Li X, Wu G. GSK3B overexpression alleviates posttraumatic osteoarthritis in mice by promoting DNMT1-mediated hypermethylation of NR4A3 promoter. Dis Markers. 2022;2022:4185489.
- [26] Mucke J, Hoyer A, Brinks R, Bleck E, Pauly T, Schneider M, et al. Inhomogeneity of immune cell composition in the synovial sublining: Linear mixed modelling indicates differences in distribution and spatial decline of CD68+ macrophages in osteoarthritis and rheumatoid arthritis. Arthritis Res Ther. 2016;18(1):170.
- [27] Tao T, Ji YH, Shen AG, Cheng C. Role of Numbl in regulating NF-κB signaling transduction in microglial polarization and central nervous inflammation [abstract]. In: Proceedings of the 9th National Congress of Immunology; 2014 Oct 18; Jinan, China. 2014. p. 753.
- [28] Kunisch E, Fuhrmann R, Roth A, Winter R, Lungershausen W, Kinne RW, et al. Macrophage specificity of three anti-CD68 monoclonal antibodies (KP1, EBM11, and PGM1) widely used for immunohistochemistry and flow cytometry. Ann Rheum Dis. 2004;63(6):774-84.
- [29] Holness CL, Simmons DL. Molecular cloning of CD68, a human macrophage marker related to lysosomal glycoproteins. Blood. 1993;81(6):1607-13.
- [30] Zhang H, Cai D, Bai X. Macrophages regulate the progression of osteoarthritis. Osteoarthritis Cartilage. 2020;28(4):555-61.
- [31] Yasuda T. Type II collagen peptide stimulates Akt leading to nuclear factor-κB activation: Its inhibition by hyaluronan. Biomed Res Tokyo. 2014;35:193.
- [32] Ikuta F, Takahashi K, Kiuchi S, Watanabe A, Okuaki T, Oshima Y, et al. Effects of repeated intra-articular hyaluronic acid on cartilage degeneration evaluated by T1p mapping in knee osteoarthritis. Mod Rheumatol. 2021;31(4):912-18.
- [33] He Z, Bu P, Xu K. Remodeling of the pro-inflammatory microenvironment in osteoarthritis via hydrogel-based photothermal therapy. Adv Compos Hybrid Mater. 2024;7:36.

PARTICULARS OF CONTRIBUTORS:

- 1. Associate Professor, Department of Sports Medicine, Shenzhen Longhua District Central Hospital, Shenzhen, Guangdong Province, China.
- 2. Principal Investigator, Department of Medical Laboratory, Shenzhen Longhua District Central Hospital, Guangdong Medical University, Shenzhen, Guangdong Province, China.
- 3. Research Associate, Department of Medical Laboratory, Shenzhen Longhua District Central Hospital, Guangdong Medical University, Shenzhen, Guangdong Province, China.
- 4. Senior Research Associate, Department of Medical Laboratory, Shenzhen Longhua District Central Hospital, Guangdong Medical University, Shenzhen, Guangdong Province, China.
- 5. Associate Professor, Department of Traumatic Orthopaedics, Shenzhen Longhua District Central Hospital, Shenzhen, Guangdong Province, China.
- 6. Research Assistant, Department of Sports Medicine, Shenzhen Longhua District Central Hospital, Shenzhen, Guangdong Province, China.
- 7. Research Assistant, Department of Sports Medicine, Shenzhen Longhua District Central Hospital, Shenzhen, Guangdong Province, China.
- 8. Research Assistant, Department of Sports Medicine, Shenzhen Longhua District Central Hospital, Shenzhen, Guangdong Province, China.

NAME, ADDRESS, E-MAIL ID OF THE CORRESPONDING AUTHOR:

Chunpei Ou,

Associate Professor, Department of Sports Medicine, Shenzhen Longhua District Central Hospital, Shenzhen, Guangdong Province, China. E-mail: 353142532@qq.com

PLAGIARISM CHECKING METHODS: [Jain H et al.]

- Plagiarism X-checker: Jun 12, 2025Manual Googling: Jul 28, 2025
- iThenticate Software: Jul 30, 2025 (3%)

EMENDATIONS: 6

ETYMOLOGY: Author Origin

AUTHOR DECLARATION:

- Financial or Other Competing Interests: As declared above.
- Was Ethics Committee Approval obtained for this study? Yes
- Was informed consent obtained from the subjects involved in the study? NA
- For any images presented appropriate consent has been obtained from the subjects. NA

Date of Submission: May 24, 2025 Date of Peer Review: Jun 17, 2025 Date of Acceptance: Aug 01, 2025 Date of Publishing: Oct 01, 2025